Available online at www.sciencedirect.com

ScienceDirect

Russian Geology and Geophysics 55 (2014) 1223–1228

RUSSIAN GEOLOGY AND GEOPHYSICS

www.elsevier.com/locate/rgg

# Impact fracture of granite at temperatures from 20 to 500 °C

I.P. Scherbakov *, A.E. Chmel

*Ioffe Physico-Technical Institute, Fracture Physics Department, Russian Academy of Sciences, ul. Politecknicheskaya 26, St. Petersburg, 194021, Russia*

Received 11 June 2013; accepted 11 October 2013

**Abstract**

Earthquake nucleation and fracture propagation in deformed rocks generate elastic waves, within acoustic frequencies. Strain-induced acoustic waves appear both in field tectonic structures and in laboratory samples, thus making laboratory acoustic emission (AE) data from load tests suitable to interpret natural seismic processes. However, laboratory tests are commonly run at room temperature, while the natural rocks at the earthquake origin depths are as hot as hundreds of degrees centigrade. We report AE data for thermally and mechanically loaded granites subjected to impact fracture at different temperatures. The energy distribution in the time series of acoustic signals emitted from fine-grained granite fits a power law of the type of the Gutenberg–Richter relationship at temperatures from 20 to 500 °C. Medium- and coarse-grained samples behave in this way only within 300 °C but show a Poissonian (random) AE energy distribution above 300 °C.


Keywords: granite; impact fracture; acoustic emission; temperature dependence

## Introduction

Rocks in numerous laboratory fracture tests with monitoring of acoustic emission (AE) and electromagnetic (EM) radiation show power-law energy dependence of frequency (number of pulses) within a certain energy ($E$) range, similar to the logarithmic Gutenberg-Richter frequency-magnitude relationship for earthquakes: $\log_{10} N(M>) \propto -bM$, where $N$ is the number (frequency) of events with the magnitude above $M$ ($M$ being proportional to $\log_{10} E$) (Kuksenko et al., 2005; Lei and Satoh, 2007; Rabinovich et al., 2002). This similarity makes laboratory AE data suitable to interpret the natural seismicity patterns (Amitrano, 2006; Davidsen et al., 2007; Genshaft, 2009; Scholz, 1968; Smirnov et al., 1995; Zavyalov and Sobolev, 1988). The approach is more so reasonable that any large-scale rupture in stressed rocks stems from the nucleation, accumulation, and clustering of microscopic defects.

However, the conditions of laboratory compressional fracture tests differ from those of natural seismicity where earthquakes originate tens of kilometers deep at high temperatures. We studied the thermal effect on rock fracture in time series of acoustic signals emitted from granite samples of different grain sizes subjected to dynamic (shock) fracture at temperatures from 20 to 500 °C, i.e., in the range below the $\alpha \rightarrow \beta$ phase transition in quartz (573 °C).

## Experiment

The granite samples were of three grain size types: two from quarries in Finland (Rapakivi and Kuru Grey granites) with grain sizes 5–7 mm and 2–3 mm, respectively, and one Westerly granite with ~0.8 mm grains, the coarsest particles being within 1.2 mm. See Table 1 for their mineralogy and some mechanic properties.

The samples, cut out as $15 \times 20 \times 20$ mm blocks, were hit locally by a 100 g load falling from a height of 10 cm on a steel sticker on the sample surface (Fig. 1), where the impacts produced pits, about 0.5 mm deep and 1–2 mm in diameter.

Acoustic emission was monitored by a transducer fixed on the flat lateral surface of the steel sticker. The sensor placed on the sticker instead of the sample surface was actually insulated from the hot sample thus reducing the background AE from thermally-induced cracks (Keshavarz et al., 2010; Yong and Wang, 1980) not related to the external mechanic loading.

Stress values at the ADC output were saved to the PC memory at every 10 ns. The highest AE frequency was 1 MHz. Low-bandpass digital filtering at 50 kHz was applied to eliminate the signals of primary elastic waves and parasitic oscillations of the sample and the test system. The background

* Corresponding author.
*E-mail address*: Sherbakov.mhd@mail.ioffe.ru (I.P. Scherbakov)

1068-7971/$ - see front matter 
http://dx.doi.org/10.1016/j.rgg.2014.09.008

Table 1. Mineralogy and some mechanic properties of granite samples

| Granite | Mineralogy, % | | | | Density, kg/m$^3$ | Grain size, mm |
|---|---|---|---|---|---|---|
| | Orthoclase | Oligoclase | Quartz | Other | | |
| Rapakivi | 40 | 19 | 30 | 11 | 2660 | 3–5 |
| Kuru Grey | 38 | 20 | 31 | 11 | 2700 | ~ 2 |
| Westerly | 32 | 33 | 28 | 7 | 2630 | 0.8 |

acoustic noise (e.g., multiple reflections from the sample walls) was removed by amplitude discrimination. The tests were performed at temperatures from 20 to 500 °C, measured by a remote *CONDTROL IR-T4* infrared thermometer.

Figure 2 shows time series of AE signals counted since the first load–sticker contact. The shift from the origin corresponds to the travel-time through the sticker to the sample and related acoustic responses before the sensor. All time series contain several narrow peaks standing out against muchweaker signals: the peaks are associated with "macroscopic" (on the scale of a laboratory specimen) damage, while the weak signals are responses to the generation of microscopic damaged sites (hypocenters) by the shock-induced wave (Scherbakov et al., 2011). Acoustic emission lasted about 300 μs totally from the medium- and coarse-grained samples and ~600 μs from the fine-grained Westerly granite. The AE intensity (square amplitude, $A^2$) increased with temperature to become at 500 °C about ten times greater than at room temperature.

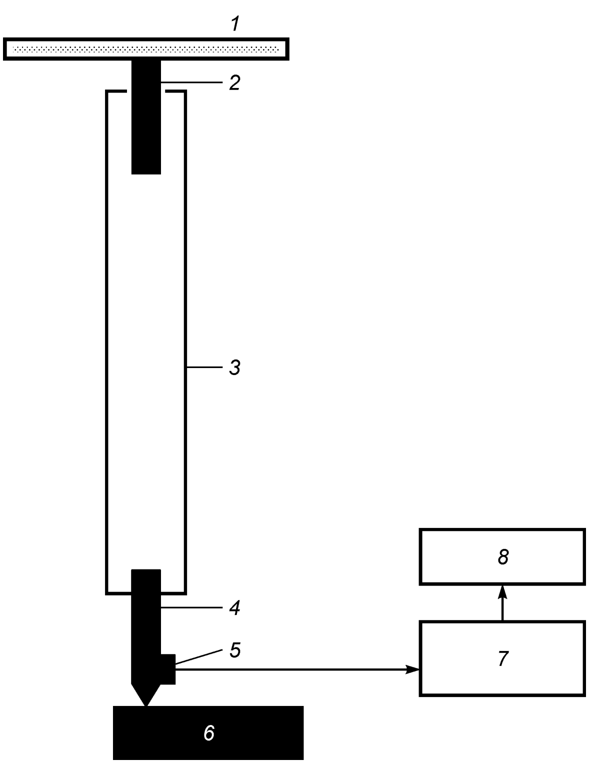


Fig. 1. Experiment layout for monitoring acoustic emission from heated granite samples subjected to impact fracture. *1*, electromagnet; *2*, load; *3*, drive; *4*, steel head; *5*, transducer; *6*, sample; *7*, ADC (ASK-3106); *8*, PC.

The AE intensity is proportional to energy release during formation of macro- and microscopic defects. Therefore, the intensity data were used to construct distributions of energy released in the events of the hypocenter nucleation and crack growth. The distributions were represented in the form of dependencies of $\log_{10} N(E > E')$, on $E'$, where $N$ is the number of AE signals corresponded to the energy exceeding the value $E'$ (Fig. 3).

The samples of coarse and medium (Rapakivi and Kuru Grey) granites show markedly different log-log energy patterns at temperatures either below or above 300 °C. Namely, below 300 °C they contain linear segments that fit the Gutenberg–Richter relationship

$$\log_{10} N(E > E') \propto -b\log_{10} E' \quad (1)$$

($\log_{10} E$ is proportional to magnitude), or in the power law form

$$\mathrm{N}(E > E') \propto E'^{-b}, \quad (1a)$$

but fail to satisfy (1) and (1a) at 400–500 °C (Fig. 3*a*, *b*). However, their semi-log $\log_{10} N(E > E')$ vs. $E'$ plots (linear along the energy axis, Fig. 4) fit well the straight lines corresponding to

$$\log_{10} N(E > E') \propto -aE' \quad (2)$$

or

$$\mathrm{N}(E > E') \propto \exp(-aE'), \quad (2a)$$

where $a$ is the constant (curve slope). The Poissonian exponential distribution (2a) indicates randomness of the AE sources.

Unlike the coarser samples, the fine Westerly granite fits the power law of (1a) over the whole temperature range (20–500 °C).

The slope of log-linear segments (parameter $b$) decreases with temperature in all samples (Table 2).

## Discussion

The power-law energy distribution (1a) means that energy release from the deformed sample remains the same at any scale because the function $N(E)$ is the only solution of the scaling equation

$$\mathrm{N}(\lambda E) = \lambda^{-b} N(E), \quad (3)$$

where $\lambda$ is the scaling exponent, and $b$ is the scaling parameter. The scale invariance is a cooperative effect arising in loaded